Neurobiology of Stress 10 (2019) 100164

Contents lists available at ScienceDirect

Neurobiology of Stress

journal homepage: www.elsevier.com/locate/ynstr

Noradrenergic depletion causes sex specific alterations in the endocannabinoid system in the Murine prefrontal cortex

M.A. Urquhart[a,1], J.A. Ross[a,*,1], B.A.S. Reyes[a], M. Nitikman[a], S.A. Thomas[b], K. Mackie[c], E.J. Van Bockstaele[a]

[a] Department of Pharmacology and Physiology, College of Medicine, Drexel University, Philadelphia, PA, 19102, USA
[b] Department of Systems Pharmacology and Translational Therapeutics, Perelman School of Medicine, University of Pennsylvania, Philadelphia, PA, 19104, USA
[c] Department of Psychological and Brain Sciences, Indiana University, Bloomington, IN, 47405-2204, USA

A B S T R A C T

Brain endocannabinoids (eCB), acting primarily via the cannabinoid type 1 receptor (CB1r), are involved in the regulation of many physiological processes, including behavioral responses to stress. A significant neural target of eCB action is the stress-responsive norepinephrine (NE) system, whose dysregulation is implicated in myriad psychiatric and neurodegenerative disorders. Using Western blot analysis, the protein expression levels of a key enzyme in the biosynthesis of the eCB 2-arachidonoylglycerol (2-AG), diacylglycerol lipase-α (DGL-α), and two eCB degrading enzymes monoacylglycerol lipase (MGL) and fatty acid amide hydrolase (FAAH) were examined in a mouse model that lacks the NE-synthesizing enzyme, dopamine β-hydroxylase (DβH-knockout, KO) and in rats treated with N-(2-chloroethyl)-N-ethyl-2-bromobenzylamine hydrochloride (DSP-4). In the prefrontal cortex (PFC), DGL-α protein expression was significantly increased in male and female DβH-KO mice ($P < 0.05$) compared to wild-type (WT) mice. DβH-KO male mice showed significant decreases in FAAH protein expression compared to WT male mice. Consistent with the DβH-KO results, DGL-α protein expression was significantly increased in male DSP-4-treated rats ($P < 0.05$) when compared to saline-treated controls. MGL and FAAH protein expression levels were significantly increased in male DSP-4 treated rats compared to male saline controls. Finally, we investigated the anatomical distribution of MGL and FAAH in the NE containing axon terminals of the PFC using immunoelectron microscopy. MGL was predominantly within presynaptic terminals while FAAH was localized to postsynaptic sites. These results suggest that the eCB system may be more responsive in males than females under conditions of NE perturbation, thus having potential implications for sex-specific treatment strategies of stress-related psychiatric disorders.

1. Introduction

Norepinephrine (NE) is a biogenic amine that has been associated with central functions such as attention, wakefulness, and the response to stress (Muntoni et al., 2006; Oropeza et al., 2007; Page, Oropeza et al. 2007, 2008). The locus coeruleus (LC) is the largest cluster of NE neurons in the brain that projects to almost all levels of the neuraxis and is the primary provider of NE to the prefrontal cortex (PFC) and hippocampus (Berridge and Waterhouse, 2003). Importantly, the LC has been implicated in a number of stress-related psychiatric disorders such as anxiety and depression, as well as neurodegenerative diseases such as Alzheimer's Disease (AD). A critical area of future research, and an endpoint of the present study, is to determine the consequences of NE depletion on neurotransmitter systems that may be potential therapeutic targets for the treatment of chronic stress-related psychiatric and neurodegenerative disorders, such as the endogenous cannabinoid (eCB) system (Carvalho et al., 2010; Van Bockstaele, 2012). This avenue of exploration is critical because damage to the LC, evident in animal models of depression, chronic stress (Nakamura, 1991; Kitayama et al., 1994; Gonzalez and Aston-Jones, 2008; Kitayama et al., 2008; Szot et al., 2016) and AD (Tomlinson et al., 1981; Bondareff et al., 1987; Forstl et al., 1992; Zarow et al., 2003; Chalermpalanupap et al., 2013; Takahashi et al., 2015), and resultant alterations in NE transmission and signaling (Wyatt et al., 1971; Schildkraut et al., 1978; Roy et al., 1988; Chan-Palay and Asan, 1989; Zubenko et al., 1990; Klimek et al., 1997; Southwick et al., 1999; Wong et al., 2000; Placidi et al., 2001; Ordway et al., 2003; Moret and Briley, 2011) may be mitigated by targeting the eCB system (Kathuria et al., 2003; Gobbi et al., 2005; Piomelli, 2005; Witkin et al., 2005a; Witkin et al., 2005b; Basavarajappa, 2007; Centonze et al., 2007; de Fonseca and Schneider, 2008; Koppel and Davies, 2008; Hill et al., 2009; Scotter et al., 2010; Carvalho and Van Bockstaele, 2012). The purpose of the present study is to understand how the eCB system may undergo concurrent alterations in response to decreased NE transmission and, to further our current understanding of how the eCB system may be targeted to treat conditions in which the LC-NE system is disrupted.

Derived from plasma membrane phospholipids, endogenous cannabinoids (eCBs) are widely distributed throughout the central nervous

* Corresponding author. Department of Pharmacology and Physiology, College of Medicine, Drexel University, 245 S. 15th Street, Philadelphia, PA, 19102, USA.
E-mail address: jar485@drexel.edu (J.A. Ross).
[1] M.A. Urquhart and J.A. Ross contributed equally to this work.

https://doi.org/10.1016/j.ynstr.2019.100164
Received 3 January 2019; Received in revised form 1 March 2019; Accepted 6 April 2019
Available online 10 April 2019

system (Freund et al., 2003; Piomelli, 2003; Chevaleyre et al., 2006). The first eCB ligand discovered was N-arachidonylethanolamide (AEA) (Devane et al., 1992), a compound synthesized by N-acyl-phosphatidylethanolamine (NAPE-PLD) (Egertova et al., 2008), and degraded by fatty acid amide hydrolase (FAAH) (Deutsch and Chin, 1993). The most abundant eCB in the mammalian brain is 2-arachidonoylglycerol (2-AG) (Mechoulam et al., 1995; Sugiura et al., 1995; Stella et al., 1997), which is synthesized in postsynaptic neurons by diacylglycerol lipase (DGL) (Bisogno et al., 2003) and degraded by monoacylglycerol lipase (MGL) (Kitaura et al., 2001). The primary mechanism proposed for 2-AG release involves a depolarization or G protein-induced 2-AG post-synaptic synthesis, followed by retrograde signaling and binding of the endogenous ligand to presynaptically distributed cannabinoid type 1 (CB1r) (Freund et al., 2003; Chevaleyre et al., 2006; Castillo et al., 2012a,b; Cathel et al., 2014). Although extensive literature supports modulation of glutamate and GABA transmission by cannabinoids, growing evidence supports their action on catecholamines, including NE.

We, among others, have previously shown that CB1r are abundantly expressed in NE- LC neurons, and may serve as a cellular substrate for modulating LC activity (Oropeza et al., 2007; Page, Oropeza et al. 2007, 2008; Castillo et al., 2012a,b). We have also provided anatomical evidence for direct synaptic associations between NE afferents in the PFC, CB1r and DGL, using high-resolution immunoelectron microscopy. DGL-α, the most abundant isoform of DGL, is localized in postsynaptic neurons that are targeted by axon terminals immunoreactive for dopamine β-hydroxylase (DβH) (Reyes et al., 2015). DβH converts dopamine to NE and represents a marker for NE neurons, as it completes the final step of NE synthesis and is present in the vesicles of NE axon terminals (Hartman et al., 1972). CB1r and DβH are co-localized presynaptically (Oropeza et al., 2007; Reyes et al., 2015), suggesting regulation of the NE afferents by the eCB system in the PFC (Reyes et al., 2015).

The eCB system modulates NE signaling primarily through CB1r (Castillo et al., 2012a,b), both in the LC and in the PFC. Several previously published studies from our group and others provide evidence for a functional link between CB1r and NE output. For example, repeated administration of the CB1r agonist WIN 55,212–2 results in increased tyrosine hydroxylase (TH) expression in the LC (Page et al., 2007), the enzyme responsible for the first and rate-limiting step of NE biosynthesis (Nagatsu et al., 1964). Further, alterations in TH expression were accompanied by increases in anxiety-like behavior (Page et al., 2007). Moreover, administration of WIN 55,212–2 results in two-fold increases in NE efflux in the PFC, an effect that is abrogated by pretreatment with the CB1r selective antagonist SR-141716 A (Oropeza et al., 2007; Page, Oropeza et al. 2007, 2008). The link between chronic cannabis use and affective disorders including anxiety, depression, cognitive impairment and psychosis is supported by several studies (Arnold et al., 2001; Degenhardt et al., 2001; Berrendero and Maldonado, 2002; Patton et al., 2002; Manzanares et al., 2004). Of particular relevance, is the finding that chronic exposure to cannabinoid agonists is associated with mood disorders including anxiety and depression (de Fonseca and Schneider, 2008; Pattij et al., 2008; Wiskerke et al., 2008), which may be, in part, an effect driven by its influence on NE.

With mounting evidence that the eCB system has profound modulatory effects on the LC-NE system, we sought to determine the effects of NE depletion on the eCB system. To accomplish this, in the present study we have employed two approaches to induce noradrenergic depletion. First, we used a genetically modified mouse model in which the DβH gene is knocked out (DβH-KO) (Thomas et al., 1995; Thomas et al., 1998). Second, we used a toxicological lesion caused by intraperitoneal injection of the LC-selective neurotoxin, N-(2-chloroethyl)-N-ethyl-2-bromobenzylamine hydrochloride (DSP-4) (Jaim-Etcheverry and Zieher, 1980) a model that has been used to recapitulate conditions of LC-specific degeneration (Heneka et al., 2002; Jardanhazi-Kurutz et al., 2010). The level of eCB tone, and consequent activity, is influenced by the balance of eCB synthesizing and degrading enzymes. To explore the protein expression of the 2-AG synthesizing and degrading enzymes under the conditions of NE depletion, DGL-α, MGL and FAAH were examined in the prefrontal cortex by Western blot analysis. These findings provide additional information for further understanding the complex interaction of eCB- and NE systems in neurological and psychiatric disorders by demonstrating that significant sex differences exist in eCB compensation in response to NE depletion.

2. Materials and methods

The procedures employed in the present study conformed to Drexel University Institutional Animal Care and Use Committee, *National Institute of Health's Guide for the Care and Use of Laboratory Animals* (1996), the Health Research Extension Act (1985) and the PHS Policy on Humane Care and Use of Laboratory Animals (1986). All efforts were made to utilize only the minimum number of animals necessary to produce reliable scientific data, and experiments were designed to minimize any animal distress.

2.1. DβH-KO mice and DSP-4 administration in rats

For Western blotting experiments, wild-type (WT) and DβH-KO littermates (3–8 months old) were housed three per cage in a controlled environment (12-h light schedule, temperature at 20 °C). In this study, there were a total of 30 mice used, 9 male WT mice, 9 male DβH-KO mice, 6 female WT mice, and 6 female DβH-KO mice. The DβH-KO mice were genetically engineered to disrupt the allele coding for DβH; therefore, these mice do not produce DβH and cannot synthesize NE (Thomas et al., 1995; Thomas et al., 1998). L-dihydroxyphenylserine (L-DOPS), a synthetic precursor to NE, was administered during embryonic development (E8.5-E19) in the pregnant female's drinking water because NE is essential to the survival of the fetus (Thomas et al., 1995). WT and DβH-KO mice were anesthetized with isoflurane (Vedco, St. Joseph, MO), then decapitated for brain extraction and microdissection.

For Western blot experiments, 14 adult male and 10 adult female Sprague-Dawley rats (Jackson Laboratory) weighing 200–250 g were used to examine the effects of DSP-4 (Sigma-Aldrich, St. Louis, MO) injections on protein expression. All rats were housed two per cage in a controlled environment (12-h light schedule, temperature at 20 °C). After a one-week acclimation period, the rats were weighed and injected intraperitoneally with 0.9% saline (females n = 4, males n = 6) or 50 mg/kg of DSP-4 in 0.9% saline (females n = 3, males n = 5) (Sigma-Aldrich, St Louis, MO). After seven days, all rats were anesthetized with isoflurane, then decapitated for brain extraction.

2.2. Analysis of estrous cycle

Female naïve rats used in baseline studies were monitored for hormonal (estrous) cycle by daily vaginal smear. Phases of estrous cycles were determined as previously described (Cora et al., 2015; Westwood, 2008). It was determined that all 3 female rats used in baseline experiments were in proestrous.

2.3. Protein extraction and western blot analysis

Brain tissues from the mice and rats were rapidly removed from each animal and placed on ice. Using a trephine, the medial PFC brain region was microdissected from each animal. The PFC was homogenized with a pestle and extracted in radioimmunoprecipitation assay (RIPA) lysis buffer (Santa Cruz Biotechnology, Santa Cruz, CA) on ice for 20 min. Lysates were cleared by centrifugation at 13,000 rpm for 12 min at 4 °C. Supernatants or protein extracts were diluted with an equal volume of Novex 2® tris glycine sodium dodecyl sulfate sample

buffer (Invitrogen, Carlsbad, CA) containing dithiothreitol (Sigma-Aldrich Inc., St. Louis, MO). Protein concentrations of the undiluted supernatants were quantified using the bicinchoninic acid protein assay reagent (Pierce, Rockford, IL).

Cell lysates containing equal amounts of protein were separated on 4–12% tris-glycine polyacrylamide gels and then electrophoretically transferred to Immobilon-P polyvinylidene fluoride membranes (Millipore, Bedford, MA). Membranes containing proteins from the medial PFC were incubated in anti-rabbit DGL-α (1:500 (Katona et al., 2006);) and mouse anti-glyceraldehyde 3-phosphate dehydrogenase (GAPDH; 1:2000; ProteinTech, Rosemont, IL, USA) primary antibodies overnight at 4 °C and then in IRdye 800CW goat anti-rabbit antibody at 1:15000 (Li-COR, Inc. Lincoln, NE, USA; P/N 926–32213) and IRdye 680LT goat anti-mouse antibody at 1:20000 (Li-COR, Inc. Lincoln, NE, USA; P/N 925–68020) for 60 min to probe for the presence of proteins. Following incubation in the secondary antibodies, blots were exposed to the Odyssey instrument (Li-COR, Inc. Lincoln, NE). DGL-α was readily detected by immunoblotting in mouse and rat PFC extracts, and was visualized as a single band that migrates at approximately 150 kDa and GAPDH as a single band that migrates at approximately 37 kDa. Blots were incubated in stripping buffer (Restore Stripping Buffer, Pierce) to disrupt previous antibody-antigen interactions and incubated in rabbit MGL (1:200 (Straiker et al., 2009);) and rabbit FAAH (1:200 (Helliwell et al., 2004);) primary antibodies overnight at room temperature and then in IRdye 800CW goat anti-rabbit antibody at 1:15000 (Li-COR, Inc. Lincoln, NE, USA; P/N 926–32213) for 60 min to probe for the presence of proteins. Following incubation in the secondary antibodies, blots were exposed to the Odyssey instrument (Li-COR, Inc. Lincoln, NE). MGL was readily detected by immunoblotting in mouse and rat PFC extracts, and was visualized as a single band that migrates at approximately 33 kDa and FAAH as a single band that migrates at approximately 63 kDa. Primary antibodies for MGL and FAAH were provided by Dr. Mackie.

2.4. Enzyme-Linked Immuno-Sorbent Assay (ELISA)

Sandwich ELISA was conducted in accordance with the instructions provided in the NE kit (NOU39-K010; Eagle, Nashua, NH). Cell lysates from 6 male and 6 female rats treated with saline or DSP-4 containing equal amounts of protein (20 μg) were used. Each sample was run in technical triplicate. A standard curve was run for each replicate and was used to estimate the concentration of NE in each sample.

2.5. Quantification

Using Image Studio Software (Li-COR, Inc. Lincoln, NE, USA), DGL-α, MGL and FAAH immunoreactivity was normalized to GAPDH immunoreactivity on each respective blot. Two-way ANOVA was used to analyze the difference in DGL-α, MGL or FAAH protein expression between WT and DβH-KO mice and male and female mice as well as in saline or DSP-treated male and female rats. All statistical analysis tests were performed using GraphPad Prism 7.03 Software (GraphPad Software, Inc. La Jolla, CA).

2.6. Tissue preparation

Male rats used for immunohistochemistry (IHC) were deeply anesthetized using isoflurane (Vedco, St. Joseph, MO) and subsequently transcardially perfused through the ascending aorta with the following fixatives: 10 ml of 1000 units/ml heparinized saline, 50 ml of 3.75% acrolein in 2% formaldehyde and 200 ml of 2% formaldehyde in 0.1 M phosphate buffer (PB) pH 7.4. Sections from the acrolein-fixed cases (n = 5) were used for immunoelectron microscopy, as acrolein fixation yields optimal tissue preservation for ultrastructural analysis. For immunofluorescence microscopy, the same procedure was conducted with 4% formaldehyde in 0.1 M PB without acrolein (n = 5). The brains were removed, cut into 4–5 mm coronal blocks, stored in 2% paraformaldehyde fixative for an additional 30 min and then sectioned (30–40 μm) on a vibrating microtome (Vibratome; Pelco EasiSlicer, Ted Pella, Redding, CA) for electron microscopy, or a cryostat (Microm HM 50, Microm International, Waldorf, Germany) for fluorescence microscopy. Brains were cut in 40 μm coronal sections, and PFC sections were selected for IHC processing using the rat brain atlas of Paxinos and Watson (Paxinos and Watson, 1986). The medial PFC was the primary region of interest selected for immunohistochemistry experiments and is imaged in the micrographs displayed in Figs. 5–8.

2.7. Immunohistochemical labeling

2.7.1. Primary antisera

Acrolein-perfused tissues were incubated in 1% sodium borohydride in 0.1 M PB to remove reactive aldehydes, and then blocked in 0.5% BSA in 0.1 M Tris-buffered saline (TBS). Tissue sections were incubated for 48 h at 4 °C in primary antibody in 0.1% BSA and 0.25% Triton X-100 in 0.1 M TBS. Triple-labeled tissues were incubated in a cocktail of rabbit anti-MGL (1:200) or rabbit anti-FAAH (1:200), guinea pig anti-CB1 (1:1000) and mouse anti-DβH (Chemicon International, Temecula, CA; 1:1000) or mouse anti-NET (MAb Technologies Inc., Stone Mountain, GA; 1:1000 (for specificity and characterization, see (Oropeza et al., 2007; Reyes et al., 2015; Scavone et al., 2010).

2.7.2. Electron microscopy

The secondary antibodies used for electron microscopy were biotinylated anti-mouse for DβH at 1:400, and 1 nm gold particle conjugated goat anti-rabbit IgG (Electron Microscopy Science, Hatfield, PA) at 1:50 for MGL or FAAH. Immunoperoxidase labeling of DβH was performed as described above. Electron-dense labeling of MGL or FAAH was detected via silver intensification of immunogold particles using a silver enhancement kit (Aurion R-GENT SE-EM kit, Electron Microscopy Science). Tissues were prepared for visualization under the electron microscope as previously described, with osmification, serial dehydration, flat-embedding, and tissue sectioning at 74 nm on an ultramicrotome (Commons et al., 2001). Sections were collected on copper mesh grids and examined using an electron microscope (Morgani, Fei Company, Hillsboro, OR). Digital images were viewed and captured using the AMT advantage HR HR-B CCD camera system (Advance Microscopy Techniques, Danvers, MA). Immunofluorescence and electron micrograph images were prepared using Adobe Photoshop to adjust the brightness and contrast.

2.7.3. Immunofluorescence

For confocal microscopy, detection of immunofluorescence-labeled antigens utilized two combinations of secondary antibodies. The first combination included secondary antibodies that were fluorescein isothiocyanate (FITC)-conjugated donkey anti-rabbit IgG (1:200; Jackson Immunoresearch) for MGL or FAAH detection; tetramethylrhodamine-5-isothiocyanate (TRITC)-conjugated donkey anti-guinea pig IgG (1:200; Jackson Immunoresearch) for CB1 detection and Cy5-conjugated donkey anti-mouse IgG (1:200; Jackson Immunoresearch) for DβH or NET detection. Tissue sections underwent serial dehydration, were mounted on slides, and coverslipped using DPX (Aldrich). Slides were then viewed using an Olympus IX81 inverted confocal microscope (Hatagaya, Shibuya-Ku, Tokyo, Japan), with helium and argon laser excitation wavelengths of 488, 543 and 635. The microscope is also equipped with filters (DM 405–44, BA505-605, and BA 560–660) and the Olympus Fluoview ASW FV1000 program. Fluorescence confocal images were assembled and adjusted for brightness and contrast in Adobe Photoshop.

2.8. Controls

Prior to dual and triple IHC experiments, antibodies were optimized

using immunoperoxidase staining and light microscopy under a variety of experimental conditions including perfusion reagents (formaldehyde or acrolein), a series of antibody dilutions, and incubation period (overnight at room temperature or 48 h at 4 °C). In addition to negative control groups that do not contain primary antibody, control groups containing primary, but no secondary were used to reveal any endogenous fluorescence or peroxidase activity. Common pitfalls of IHC have been well described (Fritschy, 2008), and have been addressed in these optimization studies. Following fixation and primary antibody incubation under the optimal conditions determined for each antibody, the tissues were subject to immunoperoxidase labeling techniques as previously described (Van Bockstaele, Colago et al., 1996). Tissues were dehydrated in a series of escalating alcohol concentrations and coverslipped with Permount (Fischer, Hampton, NH) for viewing on a light microscope (Olympus BX51, Japan, D10BXF Camera, Diagnostic Instruments, USA), or coverslipped with DPX for viewing on a confocal microscope (Olympus).

To ensure specificity of the biotinylated and gold-conjugated secondary antibodies for quantification at the ultrastructural level, control tissue taken directly from the plastic-tissue interface was processed in parallel, with omission of the primary antisera for MGL, FAAH, CB1r and DβH, and was devoid of immunolabeling. Single spurious immunogold-silver labeling may contribute to false positive labeling, indicated by the presence of single immunogold-silver particles on blood vessels, myelin or nuclei (Reyes, 2008; Van Bockstaele et al., 1996). To estimate the extent of spurious labeling, a randomized sampling of 100 myelin processes was evaluated for immunogold labeling; while spurious single gold particles were present, there was minimal labeling for 2 or more gold particles (1/100), thus a criterion of 2 or more gold particles was upheld for quantification purposes.

2.9. Ultrastructural analysis

Quantification and analysis of MGL or FAAH and DβH localization at the EM level were conducted as previously reported (Commons et al., 2001; Oropeza et al., 2007). Adequate preservation of ultrastructural morphology was one of the criteria imposed when selecting tissue sections to be used for ultrastructural analysis. A minimum of 3 sections per region of each animal from 6 animals were used for the analysis. At least 10 grids containing 4–7 thin sections each were collected from plastic-embedded sections of the PFC from each animal. Quantitative evaluation of immunoreactive elements was applied only to the outer 1–3 μm of the epon–tissue interface where penetration of antisera is optimal. To prevent the inclusion of spurious labeling in quantification, only profiles with a minimum of 2 gold particles were considered immunoreactive and used for quantification. For dual labeling, only micrographs containing both peroxidase and gold–silver markers were used for the tissue analysis to ensure that the absence of one marker did not result from uneven penetration of markers (Leranth and Pickel, 1989). Examination of serial sections was used to determine synaptic associations of axon terminals not always apparent in single sections.

Cellular elements were isolated and classified based on Fine Structure of the Nervous System (Peters and Palay, 1991). Somata were identified by the presence of a nucleus, Golgi apparatus, and smooth endoplasmic reticulum. Proximal dendrites contained endoplasmic reticulum, were apposed to axon terminals, and were larger than 0.7 μm in diameter. Synapses were verified by the presence of a junctional complex, a restricted zone of parallel membranes with slight enlargement of the intercellular space, and/or associated postsynaptic thickening. A synaptic specialization was only designated to the profiles that form clear morphological characteristics of either Type I or Type II (Gray, 1959). Asymmetric synapses were identified by thick postsynaptic densities (Gray's Type I; Gray, 1959), while symmetric synapses had thin densities both pre- and postsynaptically (Gray's Type II; Gray, 1959). An undefined synapse was defined as an axon terminal plasma membrane juxtaposed to a dendrite or soma devoid of recognizable membrane specializations and no intervening glial processes. Axon terminals were distinguished from unmyelinated axons based on synaptic vesicle presence and a diameter of greater than 0.1 μm.

Data from 6 (n = 3 male, n = 3 female) animals were used in the characterization of the anatomical substrate for eCB-NE interactions. For each animal, comparable levels of the medial PFC were selected for ultra-thin sectioning. For each animal, dendritic and axon-terminal profiles were sampled from at least 5 copper grids of ultrathin tissue sections near the tissue-plastic interface. Approximately 500 profiles from each animal were scanned, and approximately 300 of these fit all criteria below and were included in the analysis. Dendrites with a maximal cross-sectional diameter between 0.7 μm and 5 μm met the criteria for analysis, and a mix of dendrites of sizes from across this range was included in the analysis. Large profiles were excluded to avoid the bias towards positive labeling of larger structures. Extremely small, large, longitudinal and irregularly shaped profiles were excluded from the analysis due to possibly higher perimeter/surface ratios and risk of biasing the silver grain counts towards the membrane. Any profiles containing large, irregularly shaped silver grains of more than 0.25 μm were excluded from the analysis. Cellular profiles that failed to meet any of the described criteria were excluded from analysis.

3. Results

3.1. DGL-α protein expression is increased in male and female DβH-KO mice

To examine alterations of an eCB synthesizing enzyme under conditions of NE depletion, we measured DGL-α protein expression levels in the PFC of DβH-KO mice (Fig. 1). The effect of NE depletion and gender on DGL-α protein expression was analyzed using a two-way ANOVA, which revealed no significant effect for genotype (WT or DβH-KO) [$F_{1,24} = 2.8$, $p = 0.10$] or sex [$F_{1,24} = 0.98$, $p = 0.33$]. However, the interaction between factors was significant [$F_{1,24} = 16.33$, $p < 0.0005$]. In WT mice, the average DGL-α protein expression for males was 0.62 ± 0.08 and for females was 0.21 ± 0.03. In DβH-KO mice, the average DGL-α protein expression for males was 0.88 ± 0.03 and for females was 0.69 ± 0.12. Tukey's post-hoc analysis following

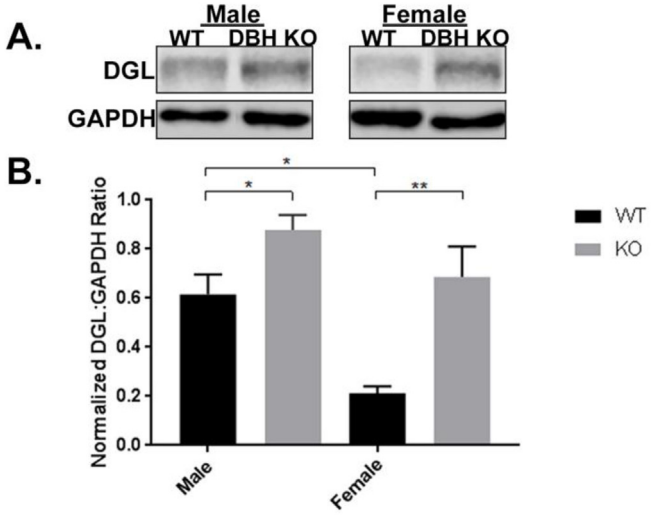

Fig. 1. Expression of Endocannabinoid-synthesizing Enzyme DGL-α in Prefrontal Cortex of wild-type (WT) and dopamine β-hydroxylase knockout (DβH-KO) male and female mice. **A.** Representative Western blot analysis shows DGL-α expression in cell lysates obtained from the PFC. **B.** DGL-α expression levels in PFC. Data are presented as mean ± SEM. Values with asterisks are significantly different ($p < 0.05$) from each other. Male WT (n = 9), female WT (n = 6), male DβH-KO (n = 9), female DβH-KO (n = 6).

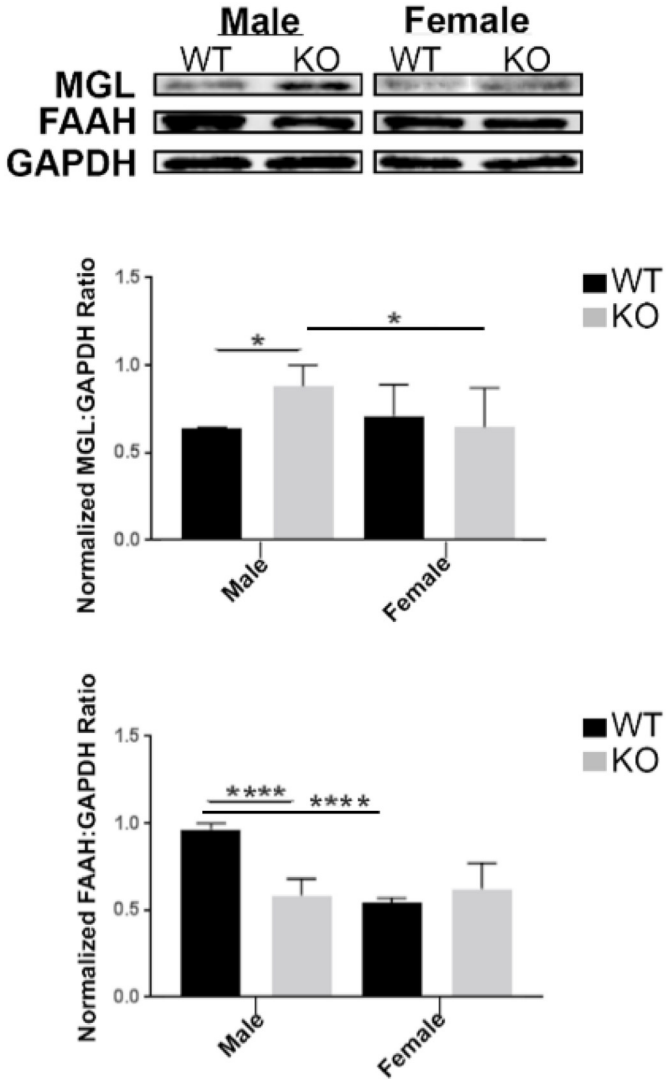

Fig. 2. Expression of Endocannabinoid-degrading Enzymes MGL, FAAH in Prefrontal Cortex of WT or DβH-KO Mice. **A.** Representative Western blot analysis shows MGL and FAAH expression. **B.** Quantification of MGL expression levels in PFC of WT or DβH-KO mice. **C.** Quantification of FAAH expression levels in PFC of WT or DβH-KO mice. Data are presented as mean ± SEM. Values with single or multiple asterisks are significantly different ($p < 0.05$, $p < 0.0001$, respectively) from each other. Tukey's multiple comparison test was run after two-way ANOVA. Male WT (n = 9), female WT (n = 6), male DβH-KO (n = 9), female DβH-KO (n = 6).

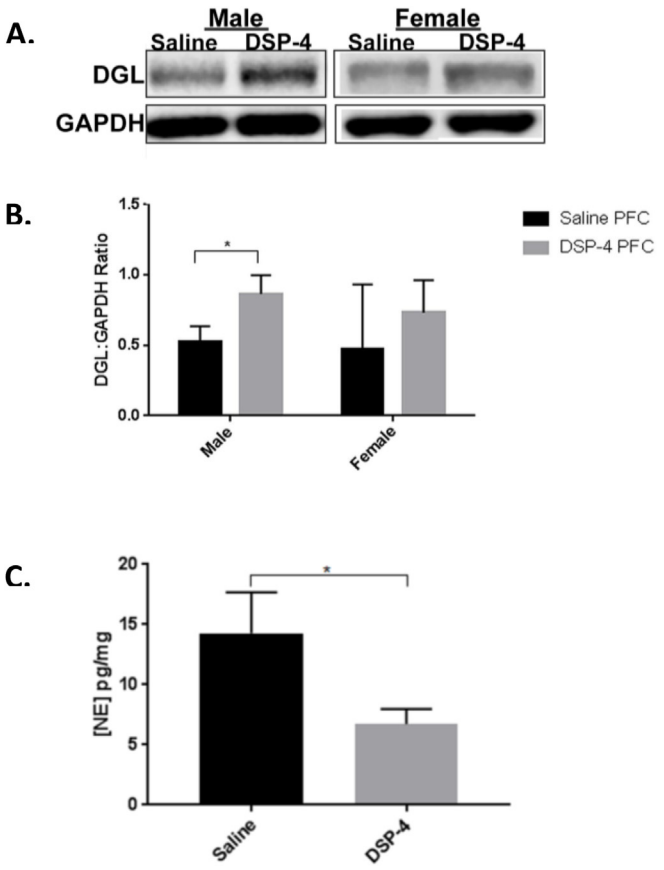

Fig. 3. Expression of Endocannabinoid-synthesizing Enzyme DGL-α in Prefrontal Cortex of Rats. DGL-α expression levels in the PFC of saline-and DSP-4-injected male and female rats. **A.** Representative Western blot analysis shows DGL-α expression in cell lysates obtained from the PFC. **B.** DGL-α expression levels in PFC. Data are presented as mean ± SEM. Values with asterisks are significantly different ($p < 0.05$) from each other. Male saline (n = 6), male DSP-4 (n = 4), female saline (n = 3), female DSP-4 (n = 3). **C.** NE expression levels in PFC. Data are presented as mean ± SEM. Values with asterisks are significantly different ($p < 0.05$) from each other. Saline (n = 6), DSP-4 (n = 6).

two-way ANOVA, as depicted in Fig. 1, showed that there were significant differences in DGL-α protein expression in the PFC between female WT and DβH-KO ($p = 0.005$), male WT and DβH-KO ($p < 0.05$), and male WT and female WT ($p < 0.05$). The significant differences in DGL-α protein expression between male WT and female WT indicate that there are initial baseline sex differences in DGL-α protein expression in the PFC in WT mice.

3.2. MGL and FAAH protein expression in DβH-KO mice

To examine alterations of eCB degrading enzymes under conditions of NE depletion, we measured MGL and FAAH protein expression levels in the PFC of DβH-KO mice (Fig. 2). In WT mice, average MGL protein expression in males was 0.64 ± 0.01 and in females was 0.71 ± 0.25. In DβH-KO mice, average MGL protein expression in males was 0.88 ± 0.16 and in females was 0.71 ± 0.25. Two-way ANOVA indicated no significant effects of sex ($F_{1,20} = 2$, $p = 0.17$), genotype ($F_{1,20} = 2.4$, $p = 0.13$), but a significant interaction between independent variables ($F_{1,20} = 7.1$, $p = 0.015$) on MGL protein expression. Tukey's post hoc analysis further identified the groups that were significantly different from each other as male WT compared to male DβH-KO ($p = 0.037$) and male DβH-KO compared to female DβH-KO ($p = 0.04$). In WT mice, average FAAH protein expression in males was 0.96 ± 0.04 and in females was 0.54 ± 0.02. In DβH-KO mice, average FAAH protein expression in males was 0.58 ± 0.09 and in females was 0.62 ± 0.15. Two-way ANOVA revealed significant effects of sex ($F_{1,20} = 33$, $p < 0.0001$), genotype ($F_{1,20} = 21$, $p = 0.0002$), and an interaction between independent variables ($F_{1,20} = 47$, $p < 0.0001$) in FAAH protein expression. Tukey's post hoc analysis further identified the groups that were significantly different from each other as male WT compared to male DβH-KO and male WT compared to female WT.

3.3. DGL-α expression is increased in male rats following DSP-4 exposure

To characterize the effect of DSP-4 treatment in terms of NE tissue concentration, a NE ELISA was conducted on samples taken from saline-treated or DSP-4-treated male and female rats (Fig. 3C). NE levels in DSP-4-treated male and female rats (6.7 pg/mg ± 1.26) were significantly reduced ($p < 0.05$) compared to saline treated rats (14.3 pg/mg ± 3.4) (Fig. 3C). DSP-4 injection resulted in a decrease to

approximately 47% of normal NE tissue concentration in the PFC. To define alterations in the eCB system under conditions of NE depletion resulting from pharmacological lesion of the LC, we examined DGL-α protein expression in the PFC (Fig. 3) following DSP-4 injection. A significant increase in DGL-α in PFC was observed in DSP-4 male rats compared to the male saline control group ($p < 0.01$). The effects of sex and treatment were analyzed using a two-way ANOVA, which revealed a significant effect of treatment ($F_{1,12} = 6.2$, $p = 0.02$) but not sex ($F_{1,12} = 0.56$, $p = 0.47$) or interaction ($F_{1,12} = 0.124$, $p = 0.73$). Post-hoc analysis revealed that DGL-α expression in male DSP-4 treated rats was significantly increased compared to male saline-treated controls ($p = 0.002$).

To investigate the possibility that there are significant differences in DGL-α levels at baseline, we also conducted Western blot analyses on PFC cell lysates of male and female naïve rats. Given the known influence of the estrous cycle in endogenous cannabinoid production, the female rats were subjected to daily vaginal smearing and were sacrificed during the proestrous phase. We examined DGL-α protein expression levels in the PFC of naïve male and female rats. There were no significant differences ($p > 0.05$) in DGL-α protein expression levels between naïve male (0.72 ± 0.14) and female (0.5 ± 0.04) rats in the PFC.

3.4. MGL and FAAH are increased in the PFC of rats treated with DSP-4

To further examine alterations in eCB degrading enzymes under conditions of NE depletion, we examined MGL and FAAH protein expression levels in the PFC of saline- or DSP-4-treated rats (Fig. 4). In saline-treated rats, the average MGL protein expression for males was 0.32 ± 0.11 and for females was 0.55 ± 0.17. In DSP-4 treated rats, the average MGL protein expression for males was 0.68 ± 0.16 and for females was 0.58 ± 0.19. The effect of NE depletion and gender on MGL protein expression was analyzed using a two-way ANOVA, which revealed significant effects of treatment ($F_{1,22} = 6.3$, $p = 0.02$), but not sex ($F_{1,22} = 0.26$, $p = 0.61$), or interaction between independent variables ($F_{1,22} = 3.8$, $p = 0.06$). Tukey's post-hoc analysis following two-way ANOVA, as depicted in Fig. 4, showed that there were significant differences in MGL protein expression in the PFC between male saline- and DSP-4-treated rats ($p < 0.05$).

The effect of NE depletion and gender on FAAH protein expression was analyzed using a two-way ANOVA, which revealed significant effects of treatment ($F_{1,19} = 18$, $p = 0.0005$), sex ($F_{1,19} = 18$, $p = 0.0004$), and interaction between independent variables ($F_{1,19} = 7.9$, $p = 0.01$). In saline-treated rats, the average FAAH protein expression in males was 0.32 ± 0.11 and in females was 0.23 ± 0.06. In DSP-4 treated rats, the average FAAH protein expression in males was 0.72 ± 0.2 and in females was 0.31 ± 0.13. Post-hoc analysis following two-way ANOVA, as depicted in Fig. 4, showed that there were significant differences in FAAH protein expression in the PFC between male saline- and DSP-4-treated rats ($p < 0.05$). There were also significant differences in male and female DSP-4-treated rats ($p < 0.05$).

3.5. MGL or FAAH, CB1r and DβH or NET localization in the PFC

Using fluorescence microscopy, MGL (Fig. 5A, D) and FAAH (Fig. 6A, D) were visualized in the PFC. MGL immunoreactivity exhibited a punctate-like appearance while FAAH immunoreactivity was evident in the processes. Immunofluorescence labeling using three distinct fluorophore-tagged secondary antibodies to localize MGL or FAAH, CB1r and DβH or NET was conducted in the same section of tissue. Immunolabeling for MGL (green labeling; Fig. 5A,E), CB1r (red labeling; Fig. 5B,F), DβH (blue labeling; Fig. 5C) and NET (blue labeling; Fig. 5G) was distributed in the PFC. MGL is localized to CB1r- and DβH-containing processes (Fig. 5A–D) or CB1r- and NET-containing processes (Fig. 5E–H)). Immunolabeling for FAAH (green labeling;

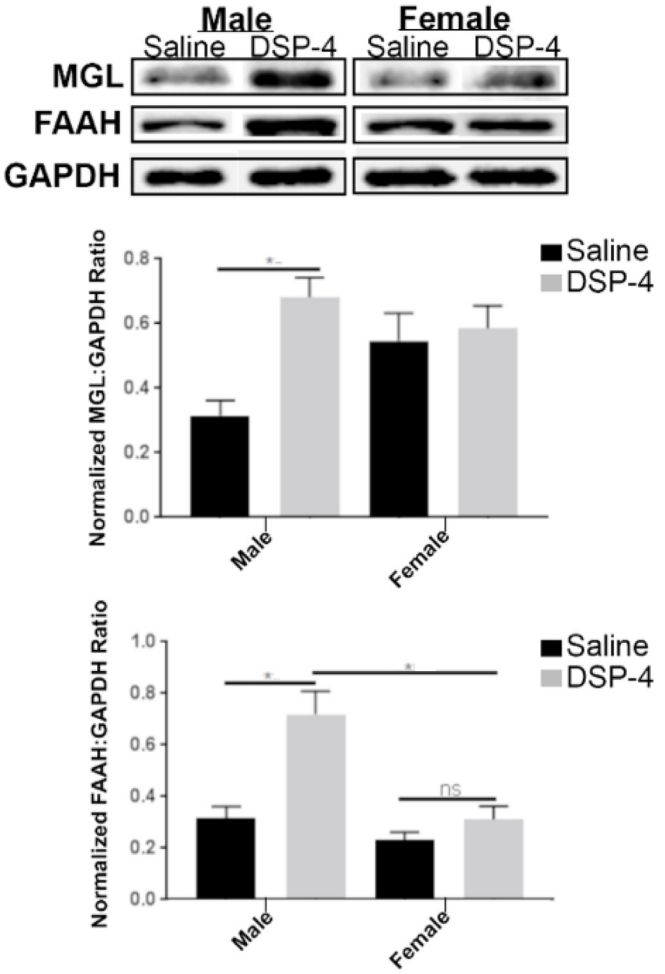

Fig. 4. Expression of Endocannabinoid-metabolizing Enzymes MGL and FAAH in Prefrontal Cortex of Rats. **A.** Representative Western blot analysis shows DGL-α expression in cell lysates obtained from the PFC of saline- or DSP-4-treated rats. **B.** DGL-α expression levels in PFC of saline- or DSP-4-treated rats. **C.** Quantification of FAAH expression levels in PFC of saline- or DSP-4-treated rats. Data are presented as mean ± SEM. Values with asterisks are significantly different ($p < 0.05$) from each other. Tukey's multiple comparison test was run after two-way ANOVA. Male WT (n = 9), female WT (n = 6), male DβH-KO (n = 9), female DβH-KO (n = 6).

Fig. 6A,E), CB1r (red labeling; Fig. 6B,F), DβH (blue labeling; Fig. 6C) and NET (blue labeling; Fig. 6G) was distributed in the PFC. FAAH immunoreactivity was evident in the processes and is localized in close proximity to CB1r- and NET-containing processes (Fig. 6E–H) or CB1r- and DβH-containing processes (Fig. 6A–D). Consistent with our previous reports (Oropeza et al., 2007; Carvalho et al., 2010; Reyes et al., 2015), DβH was localized to processes that were highly varicose and punctate in appearance. It was observed that NET immunolabeling had similar morphology, consistent with our previous reports (Carvalho et al., 2010; Reyes et al., 2015). To further define substrates for putative interactions between MGL or FAAH and DβH, putative associations were analyzed using immunoelectron microscopy.

3.6. Ultrastructural analysis of MGL and DβH in the PFC

Immunoperoxidase labeling for DβH and immunogold-silver labeling for MGL were localized in the same section of tissue in the area of interest sampled for semi-quantitative analysis (Fig. 7A–F). MGL immunogold-silver labeling was clearly distinguishable from the immunoperoxidase labeling of DβH. The area that was sampled in the PFC for electron microscopy was the same as that shown in Fig. 5 for

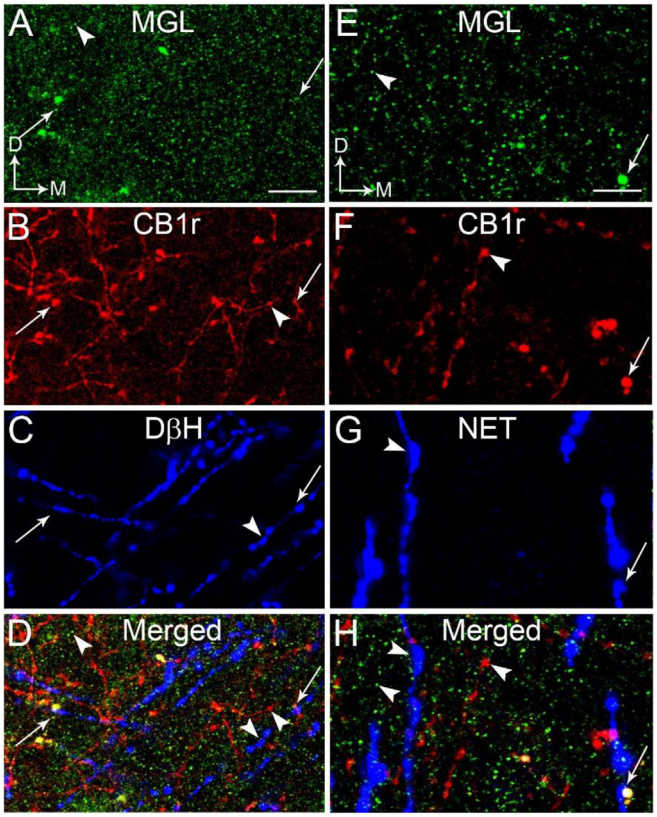

Fig. 5. A-D. Confocal fluorescence photomicrographs showing immunolabeling of monoacylglycerol lipase (MGL), cannabinoid receptor type 1 (CB1r) and dopamine beta-hydroxylase (DβH) in the frontal cortex. MGL was detected using a fluorescein isothiocyanate (FITC) donkey anti-rabbit IgG (green); CB1r was detected using a tetramethylrhodamine-5-isothiocyanate (TRITC)-conjugated donkey anti-guinea pig IgG (red) and DβH was detected using a Cy5-conjugated donkey anti-mouse IgG (blue). CB1 and DβH appeared as punctate processes. The merged image (panel D) shows colocalization of MGL, CB1r and DβH in the same process (arrows). Arrowheads indicate single-labeled MGL, CB1r or DβH. Thick arrows indicate dual labeling (MGL and DβH or CB1r and DβH). **E-H.** Confocal fluorescence photomicrographs showing immunolabeling of MGL, CB1r and norepinephrine transporter (NET) in the frontal cortex. MGL was detected using a FITC donkey anti-rabbit IgG (green); CB1r was detected using a TRITC-conjugated donkey anti-guinea pig IgG (red) and NET was detected using a Cy5-conjugated donkey anti-mouse IgG (blue). CB1r and NET appeared as punctate processes. The merged image (panel H) shows colocalization of CB1 and NET in the same process (arrows) that is in close proximity with a MGL-labeled profile. Arrowheads indicate single-labeled MGL, CB1r or NET. Thick arrows indicate dual labeling (MGL and DβH or CB1 and DβH). Scale bars: 30 μm. (For interpretation of the references to colour in this figure legend, the reader is referred to the Web version of this article.)

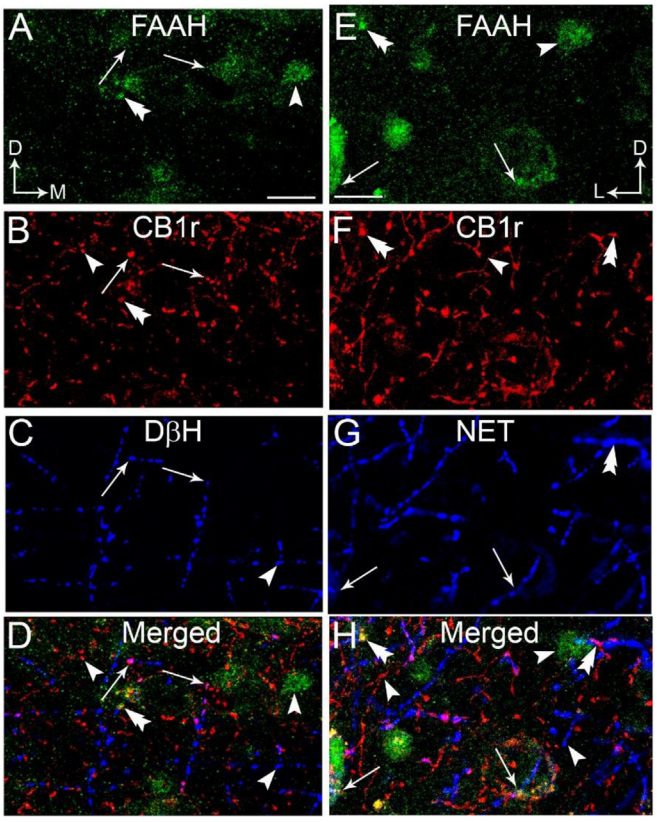

Fig. 6. A-D. Confocal fluorescence photomicrographs showing immunolabeling of fatty acid hydrolase (FAAH), CB1r and DβH in the frontal cortex. FAAH was detected using a FITC donkey anti-rabbit IgG (green); CB1r was detected using a TRITC-conjugated donkey anti-guinea pig IgG (red) and DβH was detected using a Cy5-conjugated donkey anti-mouse IgG (blue). CB1r and DβH appeared as punctate processes. The merged image (panel D) shows co-localization of CB1 and DβH in the same process (arrows) that is in close proximity with a FAAH-labeled profile (double arrowhead). **E-H.** Confocal fluorescence photomicrographs showing immunolabeling of FAAH, CB1r and norepinephrine transporter (NET) in the frontal cortex. FAAH was detected using a FITC donkey anti-rabbit IgG (green); CB1r was detected using a TRITC-conjugated donkey anti-guinea pig IgG (red) and NET was detected using a Cy5-conjugated donkey anti-mouse IgG (blue). CB1r and NET appeared as punctate processes. The merged image (panel H) shows co-localization of CB1 and NET in the same process (arrows) that is in close proximity with a FAAH-labeled profile (double arrowhead). Arrowheads indicate single-labeled FAAH, CB1r or NET. Thick arrows indicate dual labeling (FAAH and DβH or CB1 and DβH). Scale bars: 30 μm. (For interpretation of the references to colour in this figure legend, the reader is referred to the Web version of this article.)

immunofluorescence microscopy (Fig. 5, A, D). As previously demonstrated (Oropeza et al., 2007; Reyes et al., 2015), the immunoperoxidase labeling for DβH could be identified as an electron dense reaction product localized within vesicle-filled axon terminals (Fig. 7A–F). As previously reported by other groups (Miner et al., 2003; Farb et al., 2010) and our group (Oropeza et al., 2007; Reyes et al., 2015) the majority of the DβH-containing profiles was observed in unmyelinated axons and varicosities. MGL immunoreactivity detected by immunogold-silver labeling, similar to DβH, was localized primarily in the unmyelinated axons and varicosities. Immunogold-silver labeling for MGL appeared as black deposits that were distributed along the plasma membrane (Fig. 7B, D, E) and within the cytoplasmic compartment (Fig. 7A, C, D).

3.7. Ultrastructural analysis of FAAH and DβH in the PFC

Immunoperoxidase labeling for DβH and immunogold-silver labeling for FAAH were localized in the same section of tissue in the area of interest sampled for semi-quantitative analysis (Fig. 8). FAAH immunogold-silver labeling was clearly distinguishable from the immunoperoxidase labeling indicative of DβH. While the majority of DβH-containing profiles was localized in unmyelinated axons and varicosities, FAAH immunoreactivity was detected primarily in dendritic processes (Fig. 8). Clearly, DβH-containing axon terminals target FAAH-containing dendrites (Fig. 8), thus DβH labeling at the ultrastructural level was presynaptically localized with respect to FAAH-containing dendrites (Fig. 8). Targets of DβH-containing axon terminals ranged from small to large and longitudinal dendritic processes.

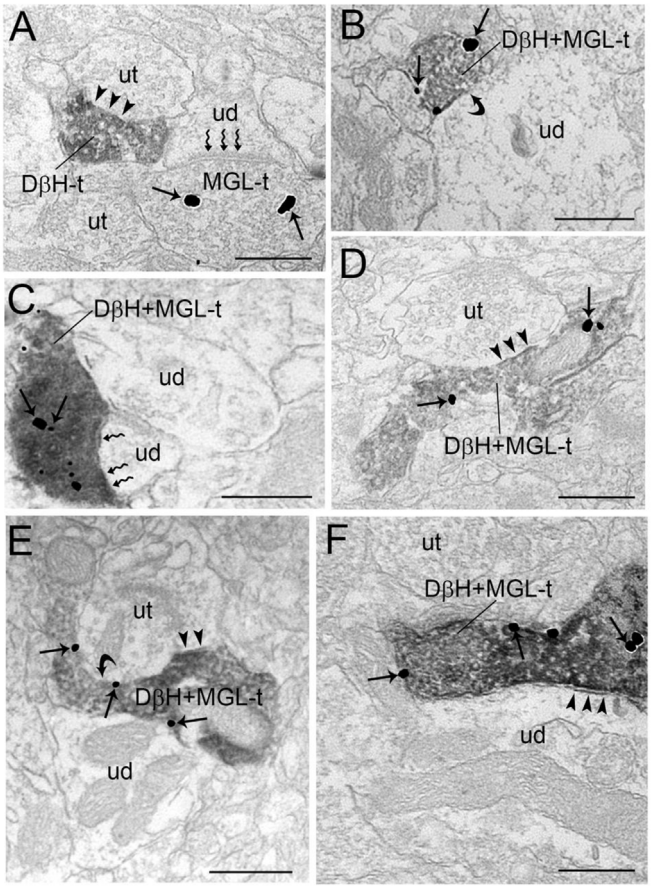

Fig. 7. Electron micrographs showing immunoperoxidase labeling for dopamine β-hydroxylase (DβH) in axon terminals and immunogold-silver labeling for monoacylglycerol lipase-α (MGL) in the prefrontal cortex. A. Immunoperoxidase labeling can be seen in a DβH-immunoreactive axon terminal (DβH-t) contacting (arrowheads) an unlabeled axon terminal. Also shown is an MGL-labeled terminal (MGL-t) that forms an asymmetric synapse (zigzag arrows) with an unlabeled dendrite (ud). B-F. Dense immunoperoxidase labeling can be seen in DβH-t that also contains MGL (DβH + MGL-t). DβH + MGL-t forms symmetric (arrowheads; Panels D and F), asymmetric (zigzag arrows; Panel C) or undefined (Panels B and E) synapse with ud. Arrows point to immunogold-silver labeling for MGL. ut: unlabeled terminal; Scale bars: 0.50 μm.

4. Discussion

Here, we examined functional and anatomical endpoints of DGL-α, MGL and FAAH that differentially act within the eCB system as they respond to circumstances in which the noradrenergic system is dysregulated. Our findings reveal interesting sex differences in adaptations to noradrenergic depletion (Table 1). In DβH-KO mice there is a global depletion of NE from birth that results in increased expression of the 2-AG synthesizing enzyme, DGL-α, in both males and females. Coupled with the finding that there was no significant change in expression of the 2-AG degrading enzyme, MGL, there may be an increase in 2-AG in the PFC of male and female DβH-KO mice, however future studies utilizing high performance liquid chromatography paired with mass spectrometry would be necessary to confirm this observation. We observed sex differences in the expression of the AEA degrading enzyme, FAAH, such that FAAH expression decreased in DβH-KO male mice and did not change in DβH-KO female mice. Taken together, these results suggest a possible increase in eCB tone of both sexes.

DSP-4-treated rats that suffer postnatal noradrenergic loss show distinct eCB changes between sexes. Male rats treated with DSP-4 may have an increase in eCB turnover, resulting from increased expression of the 2-AG-synthesizing enzyme DGL-α, as well as increased expression of the 2-AG- and AEA-degrading enzymes MGL and FAAH, respectively. Meanwhile, female rats treated with DSP-4 show no differences in DGL-α, MGL or FAAH. Given that female DβH-KO mice exhibit changes in the level of DGL-α, this could indicate that compensatory mechanisms for postnatal NE depletion are different between sexes, or that males are more eCB responsive than females to NE depletion. Compensatory responses have been described for LC neurons that survive DSP-4 lesion. These neurons attempt to restore NE tone in projection regions by increasing firing rate (Fritschy, 2008). Thus, a selective increase in firing of remaining NE neurons in the PFC in female rats could explain the lack of eCB system changes.

The functional data we report in rats treated with DSP-4 are further supported with our anatomical data in naïve rats. Corroborating the reports of others, here we show that the 2-AG-degrading enzyme MGL is localized presynaptically, and more specifically, on terminals that also exhibit DβH, the NE synthesizing enzyme or NET. Previous reports utilized northern blot and in situ hybridization to characterize the distribution of MGL mRNA transcripts in the cortex, identifying the highest concentrations in layers IV, V and VI (Dinh et al., 2002; Gulyas et al., 2004).We previously reported anatomical evidence indicating that DGL-α is localized postsynaptically, and this is consistent with the putative retrograde signaling of 2-AG that is initiated at the postsynaptic site by DGL-α and terminated at the presynaptic site by MGL following CB1r activation. In contrast to 2-AG, AEA is thought to act as an autocrine signaling molecule to regulate tonic eCB signaling. Our functional and anatomical data indicate that in naïve rats, the AEA-degrading enzyme, FAAH, is localized postsynaptically to DBH or NET containing axon terminals. These observations are in line with previously published ultrastructural studies on the subcellular localization of FAAH that focused on the hippocampus, cerebellum and amygdala which identify post-synaptic compartments and cytoplasmic membranes such as the mitochondria and smooth endoplasmic reticulum known to store Ca2+ as a primary site of FAAH localization (Gulyas et al., 2004). In support of these findings, Fig. 8 panel B-C and E display examples of FAAH immunolabeling that appears tethered to cytosolic membranes of the mitochondria. This anatomical evidence is consistent with the notion that Ca2+ release dictates, at least in part, the synthesis and release of eCBs and their degradation (Gulyas et al., 2004).

4.1. Functional implications

The results of our DSP-4-lesion studies confirm that NE depletion results in increased production of eCB markers, and are in line with the results of DβH-KO mouse models. These studies highlight the complexity of interplay between the NE and eCB systems, demonstrating that various degrees of noradrenergic depletion recruit specific elements of the eCB system, despite vastly different modes of disrupting LC functioning. These findings may have important implications for clinical conditions where the LC-NE system is thought to be perturbed, such as in the stress-related psychiatric disorders of anxiety and depression, and neurodegenerative conditions such as AD and multiple sclerosis (Gold, 1988; Klimek et al., 1997; Southwick et al., 1999; Leonard, 2001; Berridge and Waterhouse, 2003; Moret and Briley, 2011; McCall et al., 2015). The LC-NE system is engaged in parallel with the peripheral stress response when corticotropin releasing factor (CRF) is released onto the LC, resulting in the excitation of the soma and subsequent synthesis and release of NE at the many projection sites throughout the neuraxis (Valentino and Van Bockstaele, 2008). HPA-axis hyperactivity, downstream of CRF input, is thought to play a critical role in the etiology of stress related psychiatric disorders (Van Bockstaele, Colago et al., 1998; Reyes et al., 2008; Valentino and Van Bockstaele, 2008). Thus, systems that counteract responsivity to stress, such as the eCB system, may be important avenues of investigation to treat stress-related psychiatric disorders.

The eCB system may be a particularly advantageous target for such

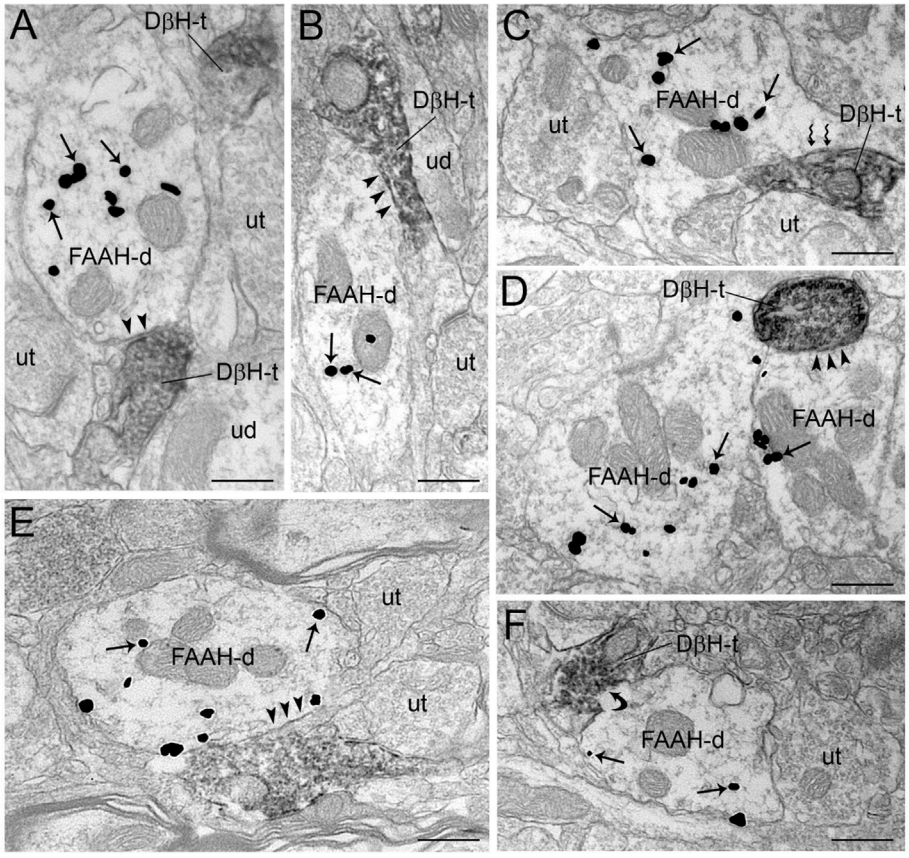

Fig. 8. Electron micrographs showing immunoperoxidase labeling for dopamine β-hydroxylase (DβH) in axon terminals and immunogold-silver labeling for fatty acid amide hydrolase (FAAH) in the prefrontal cortex. A-F. Dense immunoperoxidase labeling can be seen in a DβH-immunoreactive axon terminal (DβH-t) contacting a FAAH-labeled labeled dendrite (FAAH-d). A-B, D-E. DβH-t forms a symmetric synapse (arrowheads) with unlabeled dendrite (ud). C. A DβH-t that forms an asymmetric synapse (zigzag arrows) with a FAAH-d. F. A DβH-t forms undefined (curved arrow) synaptic contact with MGL-d. Arrows point to immunogold-silver labeling for MGL-α. ut: unlabeled terminal. Scale bars: 0.50 µm.

Table 1
Summary of alterations in eCB system resulting from NE depletion. Arrows with asterisks denotes significant alterations determined by ANOVA ($p < 0.05$), while arrow alone represents a trend that is not statistically significant.

	KO Male	KO Female	DSP-4 Male	DSP-4 Female
DGL-α	↑*	↑*	↑*	↑
MGL	No Change	No Change	↑*	No Change
FAAH	↑*	No Change	↑*	No Change

disorders because it is poised to counteract stress-responsivity in a spatially and temporally distinct manner (Hillard, 2014). Spatially, previous anatomical studies have noted that MGL and FAAH distributions are tightly overlapping with areas containing a high density of CB1r (Dinh et al., 2002). CB1 receptors are localized pre-and post-synaptically in the LC. Of particular importance are the presynaptic CB1 receptors on glutamatergic terminals, whose activation may restrain the release of excitatory amino acid neurotransmitters onto LC neurons. In LC, CB1 is expressed postsynaptically on LC-NE neurons (Scavone et al., 2010) as well as presynaptically including on glutamate terminals. CB1 is thus anatomically positioned to regulate glutamatergic drive to LC neurons, restraining their activity(Mendiguren and Pineda, 2007). Additionally, AEA acts in a spatially and temporally specific manner in that it is released tonically to restrain HPA activity in the amygdala. To initiate the stress response, AEA in the amygdala is decreased following an increase in FAAH expression levels. This results in disinhibition of excitatory afferents projecting to the hypothalamus, therefore allowing the transmission of ACTH and CRF. This response is later terminated when glucocorticoids are released into the amygdala and mediate an increase in AEA levels, thereby restoring HPA axis restraint, and preventing excessive stimulation of the stress circuit (Gunduz-Cinar et al., 2013). Thus, therapeutic approaches that harness the endogenous spatial organization and temporal responses of the eCB system, for example, FAAH or MGL inhibitors, may be particularly effective at treating stress-related psychiatric disorders.

4.1.1. Sex differences

Recent studies have found that the LC-NE arousal axis has sex differences in signaling and trafficking, particularly for corticotropin-releasing factor receptor 1 (CRFR1), that mediates stress responses (Reyes et al., 2008; Valentino et al., 2012; Valentino et al., 2013). CRFR1 signaling and trafficking could contribute to the sex differences observed in the eCB system during NE dysregulation and should be further investigated. Much of the preclinical support for this is founded on morphological (Bangasser et al., 2011), cellular (Bangasser et al., 2010), and biochemical (Valentino et al., 2013) sex differences at the CRF-LC synapse in response to stress, rendering females more responsive to prolonged stress. It is interesting to consider that male resilience to stress-related psychiatric disorders, at least in part, may be derived from the prominent role of the eCB system in males, whereas females lack the same eCB tone and responsiveness. This may allude to sexually divergent approaches to treating stress-related psychiatric disorders, as enhancing eCB tone may be more effective in alleviating stress in male, however females have stronger response to exogenous cannabinoid administration; thus, further investigation is required (Becker, 2016; Becker and Koob, 2016; Becker et al., 2017; Becker and Chartoff, 2019).

The finding that male DβH-KO mice and male rats treated with DSP-4 are more eCB responsive compared to females is consistent with our previous findings, as well as the findings of other laboratories that have investigated sex differences in the eCB system. In a recent whole-cell patch-clamp electrophysiology study conducted on LC brain sections taken from mice lacking the CB1r (CB1r-KO), it was demonstrated that male CB1r-KO mice had heightened LC-NE activity compared to female CB1r-KO mice and to WT mice. This was evident as increased NE cell excitability in male CB1r KOs, whereas there were no significant

changes in CB1r-KO females (Wyrofsky et al., 2018). Further support for the sex differences observed in this study were corroborated by NE ELISA, in which there was increased NE in CB1r-KO males compared to CB1r-KO females and WT controls (Wyrofsky et al., 2018). Additionally, other studies examining mice of both sexes that are CB1r-KO, or that are WT with the administration of CB1r antagonists, demonstrate that females do not show hypothalamic-pituitary-adrenal (HPA) axis hyperreactivity to the same degree as males (Atkinson et al., 2010; Roberts et al., 2014). Thus, the LC-NE system of females would also likely be less responsive to CB1r deletion considering that this system is activated by the HPA axis. Our studies support this rationale as we demonstrate that alterations to the noradrenergic system result in reciprocal alterations in the endocannabinoid system that are more dramatic in males compared to females.

4.1.2. Methodological considerations

Western blot analysis was conducted in parallel with ELISA studies to determine protein expression levels of the NE synthesizing enzyme, DβH, in these animals. These results were recently reported, and indicate that DβH protein expression in DSP-4-treated animals was significantly reduced compared to saline and naïve rats (Ross et al., 2017). It is possible that the effects of NE depletion on the eCB system in the PFC are indirect. Constitutive genetic deletion of DβH may produce adaptations during development that subsequently have effects on the eCB system (Thomas et al., 1998). Further, genetic deletion and DSP-4 treatment both cause systemic effects that could impact PFC function indirectly.

While DSP-4 primarily affects LC neurons, it also affects regions strongly innervated by LC neurons, such as hippocampus and dorsal raphe (Ross et al., 1973; Ross and Renyl, 1976; Ross and Stenfors, 2015). Indeed, DSP-4 is widely used in the literature as a central noradrenergic system lesion and its implications in other circuitries, such as opioid and dopaminergic circuits, as well as related noradrenergic circuits (Roczniak et al., 2016; Hauser et al., 2017, Hauser, and Knapp, 2017). A DSP-4 induced lesion provides insight into NE deficits even in these broader scenarios, due to the relative breadth of action of DSP-4. More specific mechanisms for further corroboration could be undertaken, such as investigating active noradrenergic neurons of the LC. One such mechanism would be DβH conjugated with saporin, which provide a more complete lesion compared to DSP-4. Saporin has been used this way in other studies (Carvalho et al., 2010; Ostock et al., 2014; Devoto et al., 2015), and works by binding a targeted receptor, becoming internalized, and subsequently causes downstream cell death.

5. Conclusions

Anatomical and physiological studies have confirmed the critical involvement of eCBs in a variety of physiological and pathological processes including emotional reactivity, motivated behaviors and energy homeostasis (Freund et al., 2003; Gaetani et al., 2003; Kathuria et al., 2003; Manzanares et al., 2004; Hill et al., 2009; Castillo et al., 2012a,b; Hiebel et al., 2014; Tantimonaco et al., 2014; Ceci et al., 2015; Wyrofsky et al., 2015). Our data support the hypothesis that the NE and eCB systems are intricately connected. Previous studies have demonstrated the consequences of altering eCB signaling on the LC-NE system. In the present study we aimed to determine the effects of NE depletion on the eCB system. These data add to the accumulating evidence that dysregulation of NE transmission leads to significant alterations in the eCB system, which may have profound implications for neurological and psychiatric disorders. Further investigations will help to understand the relationship of eCB regulation and the NE system in the brain and may lead to new approaches in research for potential more targeted medical applications of cannabinoids in the treatment of neurological and psychiatric disorders in the future.

Acknowledgements

This work was funded by NIH grant R01 DA020129 to EJV.

References

Arnold, J.C., Topple, A.N., Mallet, P.E., Hunt, G.E., McGregor, I.S., 2001. The distribution of cannabinoid-induced Fos expression in rat brain: differences between the Lewis and Wistar strain. Brain Res. 921 (1–2), 240–255.
Atkinson, H.C., Leggett, J.D., Wood, S.A., Castrique, E.S., Kershaw, Y.M., Lightman, S.L., 2010. Regulation of the hypothalamic-pituitary-adrenal axis circadian rhythm by endocannabinoids is sexually diergic. Endocrinology 151 (8), 3720–3727.
Bangasser, D.A., Curtis, A., Reyes, B.A., Bethea, T.T., Parastatidis, I., Ischiropoulos, H., Van Bockstaele, E.J., Valentino, R.J., 2010. Sex differences in corticotropin-releasing factor receptor signaling and trafficking: potential role in female vulnerability to stress-related psychopathology. Mol. Psychiatr. 15 (9), 896–904 877.
Bangasser, D.A., Zhang, X., Garachh, V., Hanhauser, E., Valentino, R.J., 2011. Sexual dimorphism in locus coeruleus dendritic morphology: a structural basis for sex differences in emotional arousal. Physiol. Behav. 103 (3–4), 342–351.
Basavarajappa, B.S., 2007. The endocannabinoid signaling system: a potential target for next-generation therapeutics for alcoholism. Mini Rev. Med. Chem. 7 (8), 769–779.
Becker, J.B., 2016. Sex differences in addiction. Dialogues Clin. Neurosci. 18 (4), 395–402.
Becker, J.B., Chartoff, E., 2019. Sex differences in neural mechanisms mediating reward and addiction. Neuropsychopharmacology 44 (1), 166–183.
Becker, J.B., Koob, G.F., 2016. Sex differences in animal models: focus on addiction. Pharmacol. Rev. 68 (2), 242–263.
Becker, J.B., McClellan, M.L., Reed, B.G., 2017. Sex differences, gender and addiction. J. Neurosci. Res. 95 (1–2), 136–147.
Berrendero, F., Maldonado, R., 2002. Involvement of the opioid system in the anxiolytic-like effects induced by Delta(9)-tetrahydrocannabinol. Psychopharmacology 163 (1), 111–117.
Berridge, C.W., Waterhouse, B.D., 2003. The locus coeruleus-noradrenergic system: modulation of behavioral state and state-dependent cognitive processes. Brain Res Brain Res Rev 42 (1), 33–84.
Bisogno, T., Howell, F., Williams, G., Minassi, A., Cascio, M.G., Ligresti, A., Matias, I., Schiano-Moriello, A., Paul, P., Williams, E.J., Gangadharan, U., Hobbs, C., Di Marzo, V., Doherty, P., 2003. Cloning of the first sn1-DAG lipases points to the spatial and temporal regulation of endocannabinoid signaling in the brain. J. Cell Biol. 163 (3), 463–468.
Bondareff, W., Mountjoy, C.Q., Roth, M., Rossor, M.N., Iversen, L.L., Reynolds, G.P., Hauser, D.L., 1987. Neuronal degeneration in locus ceruleus and cortical correlates of Alzheimer disease. Alzheimers Dis. Assoc. Disord. 1 (4), 256–262.
Carvalho, A.F., Mackie, K., Van Bockstaele, E.J., 2010. Cannabinoid modulation of limbic forebrain noradrenergic circuitry. Eur. J. Neurosci. 31 (2), 286–301.
Carvalho, A.F., Van Bockstaele, E.J., 2012. Cannabinoid modulation of noradrenergic circuits: implications for psychiatric disorders. Prog. Neuro-Psychopharmacol. Biol. Psychiatry 38 (1), 59–67.
Castillo, P.E., Younts, T.J., Chavez, A.E., Hashimotodani, Y., 2012a. Endocannabinoid signaling and synaptic function. Neuron 76 (1), 70–81.
Castillo, P.E., Younts, T.J., Chávez, A.E., Hashimotodani, Y., 2012b. Endocannabinoid signaling and synaptic function. Neuron 76 (1), 70–81.
Cathel, A.M., Reyes, B.A., Wang, Q., Palma, J., Mackie, K., Van Bockstaele, E.J., Kirby, L.G., 2014. Cannabinoid modulation of alpha2 adrenergic receptor function in rodent medial prefrontal cortex. Eur. J. Neurosci. 40 (8), 3202–3214.
Ceci, C., Proietti Onori, M., Macri, S., Laviola, G., 2015. Interaction between the endocannabinoid and serotonergic system in the exhibition of head twitch response in four mouse strains. Neurotox. Res. 27 (3), 275–283.
Centonze, D., Finazzi-Agro, A., Bernardi, G., Maccarrone, M., 2007. The endocannabinoid system in targeting inflammatory neurodegenerative diseases. Trends Pharmacol. Sci. 28 (4), 180–187.
Chalermpalanupap, T., Kinkead, B., Hu, W.T., Kummer, M.P., Hammerschmidt, T., Heneka, M.T., Weinshenker, D., Levey, A.I., 2013. Targeting norepinephrine in mild cognitive impairment and Alzheimer's disease. Alzheimer's Res. Ther. 5 (2), 21.
Chan-Palay, V., Asan, E., 1989. Alterations in catecholamine neurons of the locus coeruleus in senile dementia of the Alzheimer type and in Parkinson's disease with and without dementia and depression. J. Comp. Neurol. 287 (3), 373–392.
Chevaleyre, V., Takahashi, K.A., Castillo, P.E., 2006. Endocannabinoid-mediated synaptic plasticity in the CNS. Annu. Rev. Neurosci. 29, 37–76.
Commons, K.G., Beck, S.G., Rudoy, C., Van Bockstaele, E.J., 2001. Anatomical evidence for presynaptic modulation by the delta opioid receptor in the ventrolateral periaqueductal gray of the rat. J. Comp. Neurol. 430 (2), 200–208.
Cora, M.C., Kooistra, L., Travlos, G., 2015. Vaginal cytology of the laboratory rat and mouse: review and criteria for the staging of the estrous cycle using stained vaginal smears. Toxicol. Pathol. 43 (6), 776–793.
de Fonseca, F.R., Schneider, M., 2008. The endogenous cannabinoid system and drug addiction: 20 years after the discovery of the CB1 receptor. Addict. Biol. 13 (2), 143–146.
Degenhardt, L., Hall, W., Lynskey, M., 2001. The relationship between cannabis use, depression and anxiety among Australian adults: findings from the National Survey of Mental Health and Well-Being. Soc. Psychiatr. Psychiatr. Epidemiol. 36 (5), 219–227.
Deutsch, D.G., Chin, S.A., 1993. Enzymatic synthesis and degradation of anandamide, a cannabinoid receptor agonist. Biochem. Pharmacol. 46 (5), 791–796.
Devane, W.A., Hanus, L., Breuer, A., Pertwee, R.G., Stevenson, L.A., Griffin, G., Gibson,

D., Mandelbaum, A., Etinger, A., Mechoulam, R., 1992. Isolation and structure of a brain constituent that binds to the cannabinoid receptor. Science 258 (5090), 1946–1949.
Devoto, P., et al., 2015. Selective inhibition of dopamine-beta-hydroxylase enhances dopamine release from noradrenergic terminals in the medial prefrontal cortex. Brain. Behav 5 (10), e00393.
Dinh, T.P., Freund, T.F., Piomelli, D., 2002. A role for monoglyceride lipase in 2-arachidonoylglycerol inactivation. Chem. Phys. Lipids 121 (1–2), 149–158.
Egertova, M., Simon, G.M., Cravatt, B.F., Elphick, M.R., 2008. Localization of N-acyl phosphatidylethanolamine phospholipase D (NAPE-PLD) expression in mouse brain: a new perspective on N-acylethanolamines as neural signaling molecules. J. Comp. Neurol. 506 (4), 604–615.
Farb, C.R., et al., 2010. Ultrastructural characterization of noradrenergic axons and Beta-adrenergic receptors in the lateral nucleus of the amygdala. Front. Behav. Neurosci 4, 162.
Forstl, H., Burns, A., Luthert, P., Cairns, N., Lantos, P., Levy, R., 1992. Clinical and neuropathological correlates of depression in Alzheimer's disease. Psychol. Med. 22 (4), 877–884.
Freund, T.F., Katona, I., Piomelli, D., 2003. Role of endogenous cannabinoids in synaptic signaling. Physiol. Rev. 83 (3), 1017–1066.
Fritschy, J.M., 2008. Is my antibody-staining specific? How to deal with pitfalls of immunohistochemistry. Eur. J. Neurosci. 28 (12), 2365–2370.
Gaetani, S., Cuomo, V., Piomelli, D., 2003. Anandamide hydrolysis: a new target for anti-anxiety drugs? Trends Mol. Med. 9 (11), 474–478.
Gobbi, G., Bambico, F.R., Mangieri, R., Bortolato, M., Campolongo, P., Solinas, M., Cassano, T., Morgese, M.G., Debonnel, G., Duranti, A., Tontini, A., Tarzia, G., Mor, M., Trezza, V., Goldberg, S.R., Cuomo, V., Piomelli, D., 2005. Antidepressant-like activity and modulation of brain monoaminergic transmission by blockade of anandamide hydrolysis. Proc. Natl. Acad. Sci. U. S. A. 102 (51), 18620–18625.
Gold, P.W., 1988. Stress-responsive neuromodulators. Biol. Psychiatry 24 (4), 371–374.
Gonzalez, M.M., Aston-Jones, G., 2008. Light deprivation damages monoamine neurons and produces a depressive behavioral phenotype in rats. Proc. Natl. Acad. Sci. U. S. A. 105 (12), 4898–4903.
Gray, E.G., 1959. Electron microscopy of synaptic contacts on dendrite spines of the cerebral cortex. Nature 183 (4675), 1592–1593.
Gulyas, A.I., Cravatt, B.F., Bracey, M.H., Dinh, T.P., Piomelli, D., Boscia, F., Freund, T.F., 2004. Segregation of two endocannabinoid-hydrolyzing enzymes into pre- and postsynaptic compartments in the rat hippocampus, cerebellum and amygdala. Eur. J. Neurosci. 20 (2), 441–458.
Gunduz-Cinar, O., Hill, M.N., McEwen, B.S., Holmes, A., 2013. Amygdala FAAH and anandamide: mediating protection and recovery from stress. Trends Pharmacol. Sci. 34 (11), 637–644.
Hartman, B.K., Zide, D., Udenfriend, S., 1972. The use of dopamine β-hydroxylase as a marker for the central noradrenergic nervous system in rat brain. Proc. Natl. Acad. Sci. U.S.A. 69 (9), 2722–2726.
Hauser, W., et al., 2017. The opioid epidemic and national guidelines for opioid therapy for chronic noncancer pain: a perspective from different continents. Pain. Rep. 2 (3), e599.
Hauser, K.F., Knapp, P.E., 2017. Opiate Drugs with Abuse Liability Hijack the Endogenous Opioid System to Disrupt Neuronal and Glial Maturation in the Central Nervous System. Front. Pediatr. 5, 294.
Helliwell, R.J., Chamley, L.W., Blake-Palmer, K., Mitchell, M.D., Wu, J., Kearn, C.S., Glass, M., 2004. Characterization of the endocannabinoid system in early human pregnancy. J. Clin. Endocrinol. Metab. 89 (10), 5168–5174.
Heneka, M.T., Galea, E., Gavriluyk, V., Dumitrescu-Ozimek, L., Daeschner, J., O'Banion, M.K., Weinberg, G., Klockgether, T., Feinstein, D.L., 2002. Noradrenergic depletion potentiates beta -amyloid-induced cortical inflammation: implications for Alzheimer's disease. J. Neurosci. 22 (7), 2434–2442.
Hiebel, C., Kromm, T., Stark, M., Behl, C., 2014. Cannabinoid receptor 1 modulates the autophagic flux independent of mTOR- and BECLIN1-complex. J. Neurochem. 131 (4), 484–497.
Hill, M.N., Hillard, C.J., Bambico, F.R., Patel, S., Gorzalka, B.B., Gobbi, G., 2009. The therapeutic potential of the endocannabinoid system for the development of a novel class of antidepressants. Trends Pharmacol. Sci. 30 (9), 484–493.
Hillard, C.J., 2014. Stress regulates endocannabinoid-CB1 receptor signaling. Semin. Immunol. 26 (5), 380–388.
Jaim-Etcheverry, G., Zieher, L. M. a., 1980. DSP-4: a novel compound with neurotoxic effects on noradrenergic neurons of adult and developing rats. Brain Res. 188 (2), 513–523.
Jardanhazi-Kurutz, D., Kummer, M.P., Terwel, D., Vogel, K., Dyrks, T., Thiele, A., Heneka, M.T., 2010. Induced LC degeneration in APP/PS1 transgenic mice accelerates early cerebral amyloidosis and cognitive deficits. Neurochem. Int. 57 (4), 375–382.
Kathuria, S., Gaetani, S., Fegley, D., Valino, F., Duranti, A., Tontini, A., Mor, M., Tarzia, G., La Rana, G., Calignano, A., Giustino, A., Tattoli, M., Palmery, M., Cuomo, V., Piomelli, D., 2003. Modulation of anxiety through blockade of anandamide hydrolysis. Nat. Med. 9 (1), 76–81.
Katona, I., Urban, G.M., Wallace, M., Ledent, C., Jung, K.M., Piomelli, D., Mackie, K., Freund, T.F., 2006. Molecular composition of the endocannabinoid system at glutamatergic synapses. J. Neurosci. 26 (21), 5628–5637.
Kitaura, S., Suzuki, K., Imamura, S., 2001. Monoacylglycerol lipase from moderately thermophilic Bacillus sp. strain H-257: molecular cloning, sequencing, and expression in Escherichia coli of the gene. J. Biochem. 129 (3), 397–402.
Kitayama, I., Nakamura, S., Yaga, T., Murase, S., Nomura, J., Kayahara, T., Nakano, K., 1994. Degeneration of locus coeruleus axons in stress-induced depression model. Brain Res. Bull. 35 (5–6), 573–580.
Kitayama, I.T., Otani, M., Murase, S., 2008. Degeneration of the locus ceruleus noradrenergic neurons in the stress-induced depression of rats. Ann. N. Y. Acad. Sci. 1148, 95–98.
Klimek, V., Stockmeier, C., Overholser, J., Meltzer, H.Y., Kalka, S., Dilley, G., Ordway, G.A., 1997. Reduced levels of norepinephrine transporters in the locus coeruleus in major depression. J. Neurosci. 17 (21), 8451–8458.
Koppel, J., Davies, P., 2008. Targeting the endocannabinoid system in Alzheimer's disease. J. Alzheimer's Dis. 15 (3), 495–504.
Leonard, B.E., 2001. Stress, norepinephrine and depression. J. Psychiatry Neurosci. 26 (Suppl. 1), S11–S16.
Leranth, C., Pickel, V.M., 1989. Electron Microscopic Preembedding Double-Immunostaining Methods. Neuroanatomical Tract-Tacring Methods 2. L. Heimer, Zaborsky, L. Springer, Boston, MA.
Manzanares, J., Uriguen, L., Rubio, G., Palomo, T., 2004. Role of endocannabinoid system in mental diseases. Neurotox. Res. 6 (3), 213–224.
McCall, J.G., Al-Hasani, R., Siuda, E.R., Hong, D.Y., Norris, A.J., Ford, C.P., Bruchas, M.R., 2015. CRH engagement of the locus coeruleus noradrenergic system mediates stress-induced anxiety. Neuron 87 (3), 605–620.
Mechoulam, R., Ben-Shabat, S., Hanus, L., Ligumsky, M., Kaminski, N.E., Schatz, A.R., Gopher, A., Almog, S., Martin, B.R., Compton, D.R., et al., 1995. Identification of an endogenous 2-monoglyceride, present in canine gut, that binds to cannabinoid receptors. Biochem. Pharmacol. 50 (1), 83–90.
Mendiguren, A., Pineda, J., 2007. CB(1) cannabinoid receptors inhibit the glutamatergic component of KCl-evoked excitation of locus coeruleus neurons in rat brain slices. Neuropharmacology 52 (2), 617–625.
Miner, L.H., et al., 2003. Ultrastructural localization of the norepinephrine transporter in superficial and deep layers of the rat prelimbic prefrontal cortex and its spatial relationship to probable dopamine terminals. J. Comp. Neurol. 466 (4), 478–494.
Moret, C., Briley, M., 2011. The importance of norepinephrine in depression. Neuropsychiatric Dis. Treat. 7 (Suppl. 1), 9–13.
Muntoni, A.L., Pillolla, G., Melis, M., Perra, S., Gessa, G.L., Pistis, M., 2006. Cannabinoids modulate spontaneous neuronal activity and evoked inhibition of locus coeruleus noradrenergic neurons. Eur. J. Neurosci. 23 (9), 2385–2394.
Nagatsu, T., Levitt, M., Udenfriend, S., 1964. Tyrosine hydroxylase. The initial step in norepinephrine biosynthesis. J. Biol. Chem. 239, 2910–2917.
Nakamura, S., 1991. Axonal sprouting of noradrenergic locus coeruleus neurons following repeated stress and antidepressant treatment. Prog. Brain Res. 88, 587–598.
Ordway, G.A., Schenk, J., Stockmeier, C.A., May, W., Klimek, V., 2003. Elevated agonist binding to alpha2-adrenoceptors in the locus coeruleus in major depression. Biol. Psychiatry 53 (4), 315–323.
Oropeza, V.C., Mackie, K., Van Bockstaele, E.J., 2007. Cannabinoid receptors are localized to noradrenergic axon terminals in the rat frontal cortex. Brain Res. 1127 (1), 36–44.
Ostock, C.Y., et al., 2014. Effects of noradrenergic denervation by anti-DBH-saporin on behavioral responsivity to L-DOPA in the hemi-parkinsonian rat. Behav. Brain. Res. 270, 75–85.
Page, M.E., Oropeza, V.C., Sparks, S.E., Qian, Y., Menko, A.S., Van Bockstaele, E.J., 2007. Repeated cannabinoid administration increases indices of noradrenergic activity in rats. Pharmacol. Biochem. Behav. 86 (1), 162–168.
Page, M.E., Oropeza, V.C., Van Bockstaele, E.J., 2008. Local administration of a cannabinoid agonist alters norepinephrine efflux in the rat frontal cortex. Neurosci. Lett. 431 (1), 1–5.
Pattij, T., Wiskerke, J., Schoffelmeer, A.N., 2008. Cannabinoid modulation of executive functions. Eur. J. Pharmacol. 585 (2–3), 458–463.
Patton, G.C., Coffey, C., Carlin, J.B., Degenhardt, L., Lynskey, M., Hall, W., 2002. Cannabis use and mental health in young people: cohort study. BMJ 325 (7374), 1195–1198.
Paxinos, G., Watson, C., 1986. The Rat Brain in Stereotaxic Coordinates. Academic Press, New York.
Peters, A., Palay, S.L., 1991. The Fine Structure of the Nervous System: Neurons and Their Supporting Cells. Oxford University Press.
Piomelli, D., 2003. The molecular logic of endocannabinoid signalling. Nat. Rev. Neurosci. 4 (11), 873–884.
Piomelli, D., 2005. The endocannabinoid system: a drug discovery perspective. Curr. Opin. Investig. Drugs 6 (7), 672–679.
Placidi, G.P., Oquendo, M.A., Malone, K.M., Huang, Y.Y., Ellis, S.P., Mann, J.J., 2001. Aggressivity, suicide attempts, and depression: relationship to cerebrospinal fluid monoamine metabolite levels. Biol. Psychiatry 50 (10), 783–791.
Reyes, B.A., Heldt, N.A., Mackie, K., Van Bockstaele, E.J., 2015. Ultrastructural evidence for synaptic contacts between cortical noradrenergic afferents and endocannabinoid-synthesizing post-synaptic neurons. Neuroscience 303, 323–337.
Reyes, B.A., Valentino, R.J., Van Bockstaele, E.J., 2008. Stress-induced intracellular trafficking of corticotropin-releasing factor receptors in rat locus coeruleus neurons. Endocrinology 149 (1), 122–130.
Roberts, C.J., Stuhr, K.L., Hutz, M.J., Raff, H., Hillard, C.J., 2014. Endocannabinoid signaling in hypothalamic-pituitary-adrenocortical axis recovery following stress: effects of indirect agonists and comparison of male and female mice. Pharmacol. Biochem. Behav. 117, 17–24.
Roczniak, W., et al., 2016. Evaluation of the analgesic effect of morphine on models of acute nociceptive pain in rats with a central noradrenergic system lesion. Neuro. Endocrinol. Lett. 37 (3), 239–244.
Ross, J.A., Reyes, B.A.S., Thomas, S.A., Van Bockstaele, E.J., 2017. Localization of endogenous amyloid-beta to the coeruleo-cortical pathway: consequences of noradrenergic depletion. Brain Struct. Funct.
Ross, S.B., Johansson, J.G., Lindborg, B., Dahlbom, R., 1973. Cyclizing compounds. I. Tertiary N-(2-bromobenzyl)-N-haloalkylamines with adrenergic blocking action. Acta Pharm. Suec. 10 (1), 29–42.

Ross, S.B., Renyl, A.L., 1976. On the long-lasting inhibitory effect of N-(2-chloroethyl)-N-ethyl-2-bromobenzylamine (DSP 4) on the active uptake of noradrenaline. J. Pharm. Pharmacol. 28 (5), 458–459.
Ross, S.B., Stenfors, C., 2015. DSP4, a selective neurotoxin for the locus coeruleus noradrenergic system. A review of its mode of action. Neurotox. Res. 27 (1), 15–30.
Roy, A., Pickar, D., De Jong, J., Karoum, F., Linnoila, M., 1988. Norepinephrine and its metabolites in cerebrospinal fluid, plasma, and urine. Relationship to hypothalamic-pituitary-adrenal axis function in depression. Arch. Gen. Psychiatr. 45 (9), 849–857.
Scavone, J.L., Mackie, K., Van Bockstaele, E.J., 2010. Characterization of cannabinoid-1 receptors in the locus coeruleus: relationship with mu-opioid receptors. Brain Res. 1312, 18–31.
Schildkraut, J.J., Orsulak, P.J., Schatzberg, A.F., Gudeman, J.E., Cole, J.O., Rohde, W.A., LaBrie, R.A., 1978. Toward a biochemical classification of depressive disorders. I. Differences in urinary excretion of MHPG and other catecholamine metabolites in clinically defined subtypes of depressions. Arch. Gen. Psychiatr. 35 (12), 1427–1433.
Scotter, E.L., Abood, M.E., Glass, M., 2010. The endocannabinoid system as a target for the treatment of neurodegenerative disease. Br. J. Pharmacol. 160 (3), 480–498.
Southwick, S.M., Paige, S., Morgan 3rd, C.A., Bremner, J.D., Krystal, J.H., Charney, D.S., 1999. Neurotransmitter alterations in PTSD: catecholamines and serotonin. Semin. Clin. Neuropsychiatry 4 (4), 242–248.
Stella, N., Schweitzer, P., Piomelli, D., 1997. A second endogenous cannabinoid that modulates long-term potentiation. Nature 388 (6644), 773–778.
Straiker, A., Hu, S.S., Long, J.Z., Arnold, A., Wager-Miller, J., Cravatt, B.F., Mackie, K., 2009. Monoacylglycerol lipase limits the duration of endocannabinoid-mediated depolarization-induced suppression of excitation in autaptic hippocampal neurons. Mol. Pharmacol. 76 (6), 1220–1227.
Sugiura, T., Kondo, S., Sukagawa, A., Nakane, S., Shinoda, A., Itoh, K., Yamashita, A., Waku, K., 1995. 2-Arachidonoylglycerol: a possible endogenous cannabinoid receptor ligand in brain. Biochem. Biophys. Res. Commun. 215 (1), 89–97.
Szot, P., Franklin, A., Miguelez, C., Wang, Y., Vidaurrazaga, I., Ugedo, L., Sikkema, C., Wilkinson, C.W., Raskind, M.A., 2016. Depressive-like behavior observed with a minimal loss of locus coeruleus (LC) neurons following administration of 6-hydroxydopamine is associated with electrophysiological changes and reversed with precursors of norepinephrine. Neuropharmacology 101, 76–86.
Takahashi, J., Shibata, T., Sasaki, M., Kudo, M., Yanezawa, H., Obara, S., Kudo, K., Ito, K., Yamashita, F., Terayama, Y., 2015. Detection of changes in the locus coeruleus in patients with mild cognitive impairment and Alzheimer's disease: high-resolution fast spin-echo T1-weighted imaging. Geriatr. Gerontol. Int. 15 (3), 334–340.
Tantimonaco, M., Ceci, R., Sabatini, S., Catani, M.V., Rossi, A., Gasperi, V., Maccarrone, M., 2014. Physical activity and the endocannabinoid system: an overview. Cell. Mol. Life Sci. 71 (14), 2681–2698.
Thomas, S.A., Marck, B.T., Palmiter, R.D., Matsumoto, A.M., 1998. Restoration of norepinephrine and reversal of phenotypes in mice lacking dopamine beta-hydroxylase. J. Neurochem. 70 (6), 2468–2476.
Thomas, S.A., Matsumoto, A.M., Palmiter, R.D., 1995. Noradrenaline is essential for mouse fetal development. Nature 374 (6523), 643–646.
Tomlinson, B.E., Irving, D., Blessed, G., 1981. Cell loss in the locus coeruleus in senile dementia of Alzheimer type. J. Neurol. Sci. 49 (3), 419–428.
Valentino, R.J., Bangasser, D., Van Bockstaele, E.J., 2013. Sex-biased stress signaling: the corticotropin-releasing factor receptor as a model. Mol. Pharmacol. 83 (4), 737–745.
Valentino, R.J., Reyes, B., Van Bockstaele, E., Bangasser, D., 2012. Molecular and cellular sex differences at the intersection of stress and arousal. Neuropharmacology 62 (1), 13–20.
Valentino, R.J., Van Bockstaele, E., 2008. Convergent regulation of locus coeruleus activity as an adaptive response to stress. Eur. J. Pharmacol. 583 (2–3), 194–203.
Van Bockstaele, E.J., 2012. Cannabinoid receptor signaling and modulation of monoamines: implications for psychiatric and neurological disorders. Prog. Neuro-Psychopharmacol. Biol. Psychiatry 38 (1), 1–3.
Van Bockstaele, E.J., Colago, E.E., Cheng, P., Moriwaki, A., Uhl, G.R., Pickel, V.M., 1996. Ultrastructural evidence for prominent distribution of the mu-opioid receptor at extrasynaptic sites on noradrenergic dendrites in the rat nucleus locus coeruleus. J. Neurosci. 16 (16), 5037–5048.
Van Bockstaele, E.J., Colago, E.E., Valentino, R.J., 1998. Amygdaloid corticotropin-releasing factor targets locus coeruleus dendrites: substrate for the co-ordination of emotional and cognitive limbs of the stress response. J. Neuroendocrinol. 10 (10), 743–757.
Westwood, F.R., 2008. The female rat reproductive cycle: a practical histological guide to staging. Toxicol. Pathol. 36 (3), 375–384.
Wiskerke, J., Pattij, T., Schoffelmeer, A.N., De Vries, T.J., 2008. The role of CB1 receptors in psychostimulant addiction. Addict. Biol. 13 (2), 225–238.
Witkin, J.M., Tzavara, E.T., Davis, R.J., Li, X., Nomikos, G.G., 2005a. A therapeutic role for cannabinoid CB1 receptor antagonists in major depressive disorders. Trends Pharmacol. Sci. 26 (12), 609–617.
Witkin, J.M., Tzavara, E.T., Nomikos, G.G., 2005b. A role for cannabinoid CB1 receptors in mood and anxiety disorders. Behav. Pharmacol. 16 (5–6), 315–331.
Wong, M.L., Kling, M.A., Munson, P.J., Listwak, S., Licinio, J., Prolo, P., Karp, B., McCutcheon, I.E., Geracioti Jr., T.D., DeBellis, M.D., Rice, K.C., Goldstein, D.S., Veldhuis, J.D., Chrousos, G.P., Oldfield, E.H., McCann, S.M., Gold, P.W., 2000. Pronounced and sustained central hypernoradrenergic function in major depression with melancholic features: relation to hypercortisolism and corticotropin-releasing hormone. Proc. Natl. Acad. Sci. U. S. A. 97 (1), 325–330.
Wyatt, R.J., Portnoy, B., Kupfer, D.J., Snyder, F., Engelman, K., 1971. Resting plasma catecholamine concentrations in patients with depression and anxiety. Arch. Gen. Psychiatr. 24 (1), 65–70.
Wyrofsky, R., McGonigle, P., Van Bockstaele, E.J., 2015. Drug discovery strategies that focus on the endocannabinoid signaling system in psychiatric disease. Expert Opin. Drug Discov. 10 (1), 17–36.
Wyrofsky, R.R., Reyes, B.A.S., Yu, D., Kirby, L.G., Van Bockstaele, E.J., 2018. Sex differences in the effect of cannabinoid type 1 receptor deletion on locus coeruleus-norepinephrine neurons and corticotropin releasing factor-mediated responses. Eur. J. Neurosci.
Zarow, C., Lyness, S.A., Mortimer, J.A., Chui, H.C., 2003. Neuronal loss is greater in the locus coeruleus than nucleus basalis and substantia nigra in Alzheimer and Parkinson diseases. Arch. Neurol. 60 (3), 337–341.
Zubenko, G.S., Moossy, J., Kopp, U., 1990. Neurochemical correlates of major depression in primary dementia. Arch. Neurol. 47 (2), 209–214.